STATUS OF THE SOLEIL FEMTOSECOND X-RAY SOURCE

A. Nadji, F. Briquez, M.-E. Couprie, J.-C. Denard, J.-M. Filhol, P. Hollander, C. Herbeaux, M. Labat, J.-F. Lamarre, C. Laulhé, V. Leroux, J. Luning, O. Marcouillé, J.-L. Marlats, M. Meyer, T. Moreno, P. Morin, P. Prigent, S. Ravy, F. Sirotti, Synchrotron SOLEIL, Gif-sur-Yvette, France.

Abstract

An electron bunch slicing setup is being installed on the SOLEIL storage ring, based on the interaction between a laser and the electron beam. It will first provide 100 fs long X-ray pulses to two beamlines, working with soft X-rays (TEMPO) and hard X-rays (CRISTAL). The design of the wiggler modulator and the optimisation of the laser focusing optics and beam path, from the laser hutch to the inside of the storage ring tunnel and to the two beamlines are being finalised. In this paper, we will report on our setup specificities, the expected performance, and the installation status.

INTRODUCTION

An ultra short (30–50 fs FWHM) and high electric field laser pulse, co-propagating with an electron bunch (40–100 ps FWHM) in a wiggler ("modulator"), modulates the electrons energy in the interaction region ("slice") if the resonance condition:

$$\lambda_{SR} = \lambda_L = \frac{\lambda_w}{2\gamma^2}\left(1 + \frac{K^2}{2}\right) \qquad (1)$$

is fulfilled. Here, λ_{SR} is the central wavelength of the spontaneous emission emitted by the modulator, λ_L is the laser wavelength, λ_w is the wiggler period, γ is the Lorentz factor of the electrons and K the wiggler deflection parameter. Using dispersing magnetic fields or non-zero dispersion sections, this slice yields two transversely separated satellites which will radiate femtosecond X-ray pulses in an undulator ("radiator") located downstream. This technique, now dubbed "femtoslicing", was proposed [1] and experimentally demonstrated at the ALS [2] and then implemented and now routinely used at BESSYII [3], SLS [4] and ALS up-grade [5]. Probing atomic motion or magnetic properties with X-rays on a sub-picosecond time scale is a new field with the prospect of exciting scientific opportunities.

SOLEIL FEMTOSLICING SCHEME

The SOLEIL femtoslicing scheme differs from the projects mentioned above by its ability to provide the short pulses to several beamlines instead of one and by the method used to separate the slice from the core without any extra magnetic element. Only the dipole vacuum chamber by which the laser will enter into the ring will be modified and for which the call for tender has been already launched. Furthermore, the radiation emitted by the modulator will be routinely and independently used as a source for a dedicated beamline.

The femtoslicing will first be used by TEMPO and CRISTAL beamlines which are respectively interested by time resolved electron spectroscopy and diffraction in the sub-picosecond time scale. TEMPO has helical undulators (HU80 + HU44) covering a 0.05-to-1.5 keV photon energy range and CRISTAL with its in-vacuum undulator (U20) covers a 4-to-30 keV energy range. They will be followed in a second stage by applications at DEIMOS (Dichroïsm for magneto-optical spectroscopy) and GALAXIES (Inelastic X-ray scattering in the hard X-ray range) beamlines. The femtoslicing laser will also be used in pump- (X-ray) probe experiments and for the development of a femtosecond High Harmonic Generation (HHG) source in the VUV domain. A promising application still under study would also allow producing soft X-ray femtosecond Coherent Synchrotron Radiation by using the principle of EEHG [6].

The setting up of the SOLEIL femtoslicing scheme takes advantage of non-zero horizontal dispersion in all the storage ring straight sections. The electrons receiving the energy modulation in the modulator start betatron oscillations around a new orbit (behaving like Touschek-scattered particles). Bending magnets downstream from the modulator produce the horizontal displacements of off-energy electrons. At the radiators location, the electrons transverse position is given by the linear transport matrix from the modulator to the radiator. The sliced beam trajectory is shown (blue trace) in Figure 1.

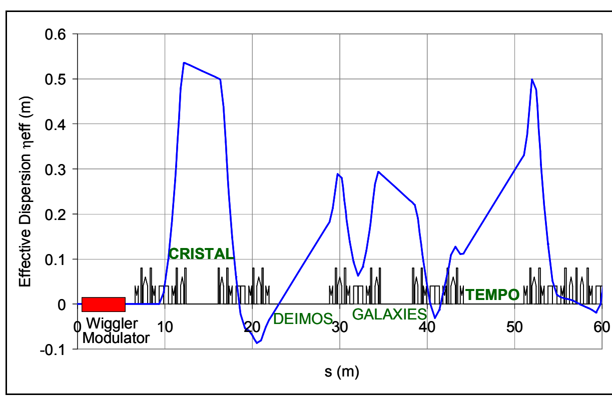

Figure 1: Trajectory of the sliced beam

The transverse displacement of the sliced beam $\Delta x(s) = \eta_{eff}(s) * \Delta E/E_0$ at each radiator depends on the local value of the effective dispersion η_{eff} [7] and on the amplitude of the energy modulation which will be discussed below.

LASER-ELECTRON INTERACTION

It is very important to optimise the interaction efficiency, especially in our case. The electron energy (2.75 GeV) is the highest and there is no easy or dedicated "knob" to increase η_{eff}. The interaction efficiency depends critically on laser performance, wiggler characteristics as well as the spectral, longitudinal and transverse overlap between laser and electron beams. With a laser beam waist exceeding the horizontal and vertical electron beam sizes, the amplitude of the energy modulation is given by [8]:

$$\Delta E\left(q,\nu,\hat{\sigma}_\tau\right)=\frac{2}{mc^2}\sqrt{A_L\alpha\hbar\omega_{0s}\frac{K^2}{2+K^2}}\,\{JJ\}f\left(q,\nu,\hat{\sigma}_\tau\right) \qquad (2)$$

where details about the expression of $\{JJ\}$ and $f\,()$ can be found in the same reference. A_L is the laser pulse energy, α is the fine structure constant, $\hbar$ is the Planck constant, ω_{0s} is the central frequency of the field of spontaneous emission. $q = L_w / z_0$, where L_w is the length of the wiggler and z_0 is the Rayleigh length. $\nu = N_w 2\delta\gamma/\gamma$; with N_w the number of periods and $\delta\gamma/\gamma$ the energy dispersion; $\hat{\sigma}_\tau = \sigma_\tau/\tau_0$, with σ_τ the rms length of the laser pulse; $\tau_0 = 2\pi N_w / kc$ where k is the wave number of the laser field.

The analytical expression (2) has been used for studying the influence of the different parameters on the amplitude of the energy modulation. It shows a monotonous increase of ΔE with the increase of the laser pulse energy and the decrease of the laser pulse duration. This emphasizes the importance of having a laser with the highest possible performance (see table 1). In the other hand, the study indicated that the Rayleigh length is a key factor for optimising the energy exchange. For example (Figure 2), a 770 mm Rayleigh length optimum is found in case of a 5 mJ laser with a 2 m long wiggler. This optimum becomes 1.05 m if the wiggler is lengthened to 3 m.

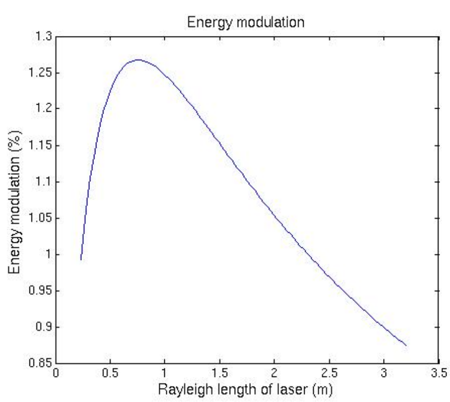

Figure 2: Variation of the energy modulation with the laser Rayleigh length.

The bandwidth ratio $\Delta\lambda_L/\Delta\lambda_W$ of laser and wiggler radiation is roughly given by $N_W/N_L \le 1$, the ratio of wiggler periods and optical cycles. If $N_W > N_L$, the electron slippage exceeds the laser pulse length and there is no further gain. Numerical simulations are carried out, using Genesis code [9], for more accurate conclusions.

THE LASER SYSTEM

The call for tender has been launched in March 2010 and the kick-off meetings for selecting the bidder will start very soon. The laser system main requirements are shown in Table 1.

Table 1: Main Requirements for the Slicing Laser System

Central wavelength **(nm)**	**800 Titanium:Sapphire**
Minimum pulse duration (FWHM) **(fs)**	**30**
Output energy @800nm **(mJ)**	**5**
Repetition rate **(kHz)**	**10**

The slicing laser hutch location has been identified (see Fig. 3). It will be in the inside gallery near the storage ring. The laser will enter the storage ring tunnel by the inner shielding wall. For pump-probe experiments, the laser is also transported to TEMPO and CRISTAL laser hutches as well as to the hutch which will host the HHG experiment. The use of several spatially separated laser systems is the reason why SOLEIL considers using only one oscillator, the one of the slicing laser system, to inject the amplifiers of the three laser systems. The design and the optimisation of the laser focusing optics from the slicing laser hutch to the four points are under finalisation.

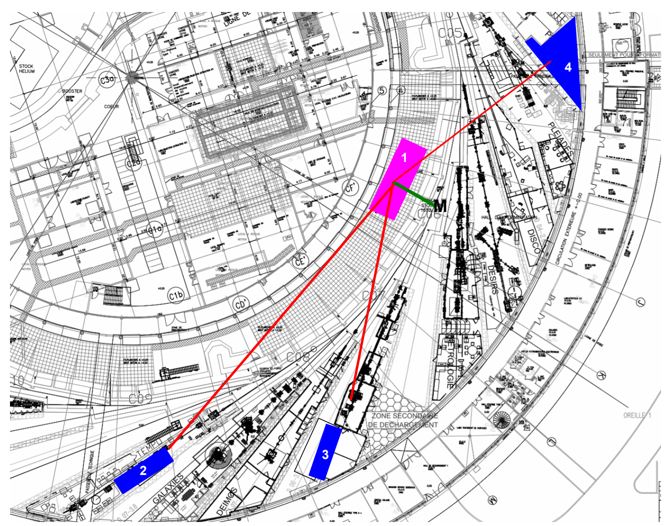

Figure 3: Slicing laser hutch location (1) and schematics transport of the laser to the wiggler modulator (M), TEMPO (2), CRISTAL (3) and HHG experiments (4).

MODULATOR WIGGLER

In order to optimize the energy exchange between laser and the electron beams, the modulator has to operate at the laser wavelength (800 nm). Figure 4 shows the 3D design and the magnetic field of the proposed modulator. It is an out-vacuum planar wiggler with a period length of 150 mm and 20 full periods including end poles, with a minimum gap of 11 mm. The number of periods is optimum for an 800 nm wavelength and 50 fs FWHM pulse duration laser. The amplitudes of the first and third harmonics of the magnetic field are respectively 1.94 T and 0.4 T at minimum gap. Each period consists of vanadium permendur poles (saturation field: 2.35 T), and NdFeB permanent magnets (VACODYM 837TP at 1.37 T represented in orange). Side magnets (VACODYM 837TP at 1.37 T in pink) with transverse magnetization are installed at both sides of the poles to enforce the field at the corners and to limit the roll-off of the field.

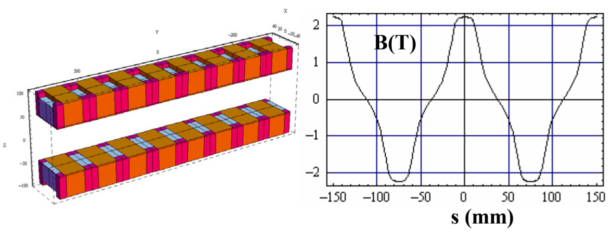

Figure 4: 3D model of 4 periods and corresponding magnetic field.

DIAGNOSTICS

Two diagnostics beamlines are planned to optimise and control in real time the laser-electron interaction efficiency. During the commissioning stage and after each shut down, the initial alignment of the laser will be performed using a retractable mirror located at the 0° wiggler exit. It will extract visible and IR radiation. Because of the high power from the wiggler (~20 kW), the optimisation will be carried out at low electron beam current and then the mirror will be moved out. At the present stage, only CCD camera and photo diodes are foreseen for optimising the timing which means that these diagnostics will be installed inside the tunnel with no need for a new hutch. For a feedback control of the energy modulation, it is planned to use the coherent THz pulse emitted downstream of a bending magnet by the "hole" created in the electron bunch by the slicing process. THz radiation will be detected using a liquid-He cooled bolometer and photo diodes in order to benefit from their complementary characteristics.

EXPECTED PERFORMANCE

The duration of the pulse produced in each radiator is determined by the duration of the laser pulse, by the slippage of the electrons with respect to the light in the wiggler, and by the effect of the emittance and energy dispersion of the electron beam. The total pulse duration at CRISTAL and TEMPO beamlines, shown in table 2, is obtained by adding quadratically these contributions. The slippage is given by $N_W\lambda_L/c \approx 53$ fs.

Table 2: Duration of the Pulse (FWHM in fs).

Radiator	Laser	Slippage	Emittance	Energy	Total
CRISTAL	50	53	54	52	104
TEMPO	50	53	47	117	145

The accurate performance in terms of number of photons issued from the slice on the sample and signal to noise ratio is still under study. Nevertheless, preliminary results are already available in [7] and updated here using the new laser parameters and the actual locations of beamline equipments. The example of CRISTAL is shown in Figure 5. A horizontal separation scheme using slits will be used. Consequently, some modifications are needed in the front end to assure the possibility to work alternatively with the horizontally shifted slice and the normal centred beam. The opening of the fixed absorber will be enlarged and the movement range of the diaphragm will be increased. The primary slits are located at 17 m from the middle of the straight section. The expected number of photons on the sample at 7 keV is about 4 10^5 photons/s.

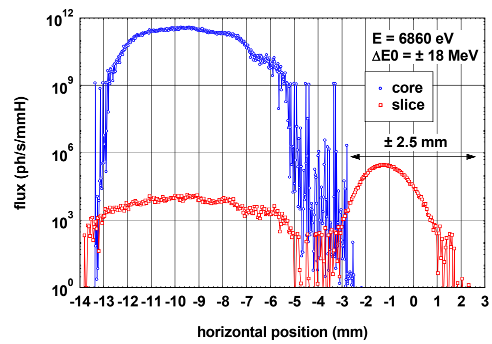

Figure 5: Expected photon flux on the sample for CRISTAL beamline.

Halo background in laser electron interaction has been calculated by A. Streun for SLS and SOLEIL [10]. At a 10 kHz laser repetition rate both CRISTAL and TEMPO can achieve a total slicing efficiency near 10^{-8}, however at a rather large halo background of 25% and 75% of the signal, respectively. Accepting a lower efficiency of 10^{-9} would reduce the background to 4%.

CONCLUSION

The technical implementation of the femtoslicing setup at SOLEIL is along the way. It is expected that two beamlines will produce femtosecond undulator radiation by the end of 2011.

ACKNOWLEDGEMENT

A. Nadji would like to thank A. Streun for his valuable calculation of the halo effect in the SOLEIL case.

REFERENCES

[1] A. Zholents and M. Zoloterev, PRL.76 (1996), 912.
[2] R. W. Schoenlein et al. Science 287 (2000), 2237.
[3] S. Khan, H. A. Dürr, EPAC'02, Paris, p. 700.
[4] G. Ingold et al., PAC'01, Chicago, p. 2656.
[5] C. Steier et al., PAC'03, Portland, p. 730.
[6] C. Evain et al., these proceedings.
[7] A. Nadji et al. EPAC'04, Lucern, p. 2332.
[8] A. A.Zholents & K. Holldack, FEL'06, Berlin, p 725.
[9] S. Reiche, NIM, A 429, 243 (1999).
[10] A. Streun, SLS-TME-TA-2010-0320.